

## Article

# Prospect of SnO<sub>2</sub> Electron Transport Layer Deposited by Ultrasonic Spraying

Wu Long <sup>1</sup>, Aoxi He <sup>1</sup>, Shenghui Xie <sup>1</sup>, Xiutao Yang <sup>1</sup> and Lili Wu <sup>1,2,\*</sup>

<sup>1</sup> College of Materials Science and Engineering, Sichuan University, Chengdu 610065, China; longwu@stu.scu.edu.cn (W.L.); heaoxi@outlook.com (A.H.); 18848253924@163.com (S.X.); yangxiutao532624@foxmail.com (X.Y.)

<sup>2</sup> Engineering Research Center of Alternative Energy Materials & Devices, Ministry of Education, Chengdu 610065, China

\* Correspondence: wulili@scu.edu.cn

**Abstract:** The SnO<sub>2</sub> electron transport layer (ETL) has been characterized as being excellent in optical and electrical properties, ensuring its indispensable role in perovskite solar cells (PSCs). In this work, SnO<sub>2</sub> films were prepared using two approaches, namely, the ultrasonic spraying method and the traditional spin-coating, where the different properties in optical and electrical performance of SnO<sub>2</sub> films from two methods were analyzed by UV-Vis, XRD, AFM, and XPS. Results indicate that the optical band gaps of the sprayed and the spin-coated film are 3.83 eV and 3.77 eV, respectively. The sprayed SnO<sub>2</sub> film has relatively low surface roughness according to the AFM. XPS spectra show that the sprayed SnO<sub>2</sub> film has a higher proportion of Sn<sup>2+</sup> and thus corresponds to higher carrier concentration than spin-coated one. Hall effect measurement demonstrates that the carrier concentration of the sprayed film is  $1.0 \times 10^{14} \text{ cm}^{-3}$ , which is slightly higher than that of the spin-coated film. In addition, the best PSCs efficiencies prepared by sprayed and spin-coated SnO<sub>2</sub> films are 18.3% and 17.5%, respectively. This work suggests that the ultrasonic spraying method has greater development potential in the field of flexible perovskite cells due to its feasibility of large-area deposition.



**Citation:** Long, W.; He, A.; Xie, S.; Yang, X.; Wu, L. Prospect of SnO<sub>2</sub> Electron Transport Layer Deposited by Ultrasonic Spraying. *Energies* **2022**, *15*, 3211. <https://doi.org/10.3390/en15093211>

Academic Editor: Kun-Mu Lee

Received: 16 March 2022

Accepted: 25 April 2022

Published: 27 April 2022

**Publisher's Note:** MDPI stays neutral with regard to jurisdictional claims in published maps and institutional affiliations.



**Copyright:** © 2022 by the authors. Licensee MDPI, Basel, Switzerland. This article is an open access article distributed under the terms and conditions of the Creative Commons Attribution (CC BY) license (<https://creativecommons.org/licenses/by/4.0/>).

## 1. Introduction

Organic–inorganic hybrid perovskite solar cells (PSCs) have excellent photovoltaic performance and low manufacturing costs, and the power conversion efficiency (PCE) has rapidly increased from 3.8% in 2009 to 25.5% in 2021 [1–6]. High absorption coefficient [7], low trap-state density [8], and convenient solution preparation process [9] have led to its great potential, which also includes the role of a suitable electron transport layer (ETL) SnO<sub>2</sub>. SnO<sub>2</sub> has a wide band gap (3.6–4.5 eV) [10], high light transmittance [11], high electron mobility, good energy-level matching with the perovskite absorption layer [12], and low-temperature processability. In recent years, it has been widely used in the ETL of perovskite solar cells. There are many methods for preparing SnO<sub>2</sub> thin films, including spin-coating [13], chemical vapor deposition (CVD) [14], atomic layer deposition (ALD) [15], sputtering [16], spray pyrolysis [17], etc. Using the spin-coating method makes it difficult to control the uniformity of large-area thin films. The sputtering method requires a vacuum environment. The ALD preparation method can be prepared in a large area, but the cost is too high and it is difficult to expand. The spray pyrolysis method requires high-temperature heating of the substrate, which makes it difficult to apply to flexible perovskite cells. Therefore, we adopted a simple method with high feasibility at low temperature—ultrasonic spraying to prepare SnO<sub>2</sub> thin films.

The ultrasonic spraying method is a rapid-deposition method that can prepare SnO<sub>2</sub> thin films in a large area at room temperature. For example, in 2018, Mahmood et al.

used electrospray technology to prepare  $\text{SnO}_2$  films for  $\text{MAPbI}_3$  cells and obtained 15.69% PCE [18]. Recently, Taheri et al. used sprayed  $\text{Np-SnO}_2$  as the ETL, and solar cells based on  $\text{MAPbI}_3$  showed a maximum PCE of 16.77% [19]. Bishop et al. used ultrasonic spraying to deposit  $\text{SnO}_2$  film, trication perovskite, and Spiro-OMeTAD, and prepared a perovskite solar cell with the best PCE of 19.4%. They obtained the best PCE of 16.3% by full spraying on a large-area substrate of 25 mm × 75 mm [20]. Although there have been many studies on ultrasonic spray deposition of  $\text{SnO}_2$  thin films and preparation of perovskite cells based on this, most of these studies are based on ITO substrates with low surface roughness. At present, there are few reports on the  $\text{SnO}_2$  film based on FTO substrate. Compared with ITO substrate, FTO substrate does not need to be doped with the rare metal indium, and possibly has better interface matching with ETL of  $\text{SnO}_2$  due to the same material.

Spin-coating is not suitable for large-area film deposition due to its non-uniformity, while the spray method is optimal for large-area deposition. Therefore, in this work, we used the same  $\text{SnO}_2$  raw material ( $\text{SnO}_2$  (15 wt.% in  $\text{H}_2\text{O}$  colloidal dispersion)) to prepare film by spin-coating and spraying. The properties of the films prepared by the two methods were characterized. Then, the performances of perovskite solar cells based on the two kinds of  $\text{SnO}_2$  films were compared to find out whether spraying method has potential to take the place of the spin-coating method in the large-area production of perovskite modules.

## 2. Experiment

### 2.1. Materials

FTO-coated glass substrates (Tec10, 9.6  $\Omega/\text{sq}$ ) were purchased from Pilkington Group Limited (Shanghai, China).  $\text{SnO}_2$  (15% in  $\text{H}_2\text{O}$  colloidal dispersion) was purchased from Alfa Aesar (Alfa Aesar (China) Chemical Co., Ltd., Shanghai, China). Sigma-Aldrich (Sigma-Aldrich (Shanghai) Trading Co., Ltd., Shanghai, China) provided dimethyl sulfoxide (DMSO, anhydrous, >99.5%), *N,N*-dimethylformamide (DMF, anhydrous, 99.8%), acetonitrile (anhydrous, 99.8%), isopropanol (IPA, anhydrous, 99.5%), chlorobenzene (CB, anhydrous, 99.8%), bis(trifluoromethane)sulfonimide lithium salt (Li-TFSI, 99.95%), and 4-tert-butylpyridine (tBP, 96%). Lead iodide ( $\text{PbI}_2$ , 99.99%) was purchased from TCI. FAI (≥99.95%),  $\text{MCl}$  (≥99.95%),  $\text{CsI}$  (>99.99%),  $\text{FABr}$  (≥99.95%),  $\text{MABr}$  (≥99.95%), and 2,2',7,7'-tetrakis[*N,N*-di(4-methoxyphenyl)-amino]-9,9'-spiro-bifluorene (Spiro-OMeTAD, ≥99.8%) were provided by Xi'an Polymer Light Technology Corp. (Xi'an, China). Beijing Licheng Innovation Metal Material Technology Co. Ltd. (Beijing, China) provided Au (99.999%). All materials were used as received, without subsequent processing or further purification.

### 2.2. Preparation of $\text{SnO}_2$ Thin Films

Tec10 glass was immersed in Amway cleaner (Amway home Multi-Purpose Cleaner, Amway (China) Commodity Co., Ltd. Guang Zhou, China.), ultrasonically cleaned with deionized water, and dried. Before ultrasonic spraying, the substrate was treated with UV-ozone (UVO CLEANER, Model No. 342-220, Jelight Company Inc. Irvine, CA, USA) for 15 min. The  $\text{SnO}_2$  raw material was diluted with 18  $\text{M}\Omega$  deionized water, and a small amount of absolute ethanol was added during dilution to speed up the evaporation of the solvent during annealing. The  $\text{SnO}_2$  precursor was prepared by mixing  $\text{SnO}_2$  colloidal dispersion, deionized water, and absolute ethanol at a volume ratio of 1:40:10, and we aspirated the precursor with a disposable syringe and filtered it through a 0.22  $\mu\text{m}$  pore size Teflon filter after 20 min of stirring.

The equipment model of the ultrasonic atomization system is Perfect ·Coat, provided by Zhenzhi Nano-coating Equipment Co., Ltd., Guangzhou, China. We sprayed  $\text{SnO}_2$  on the substrate at room temperature with the nozzle height of 40 mm, the nozzle moving speed of 25 mm/s, and the spraying pressure of 0.1 MPa. The spraying time was 36 s, and the size of the substrate was 2.5 × 2.5  $\text{cm}^2$ . After spraying, the substrate was immediately transferred to a heated plate at 180 °C and annealed for 20 min [21–23]. The thickness of the film was about 20 nm. The spraying and spin-coating films are obtained from solutions of

the same starting substances. The  $\text{SnO}_2$  precursor was prepared by mixing  $\text{SnO}_2$  colloidal dispersion and deionized water at a volume ratio of 1:3. A total of 100  $\mu\text{L}$  of  $\text{SnO}_2$  precursor was spin-coated at 4000 rpm for 20 s. Then, the substrate was annealed at 180 °C for 20 min [24].

### 2.3. Preparation of the Device

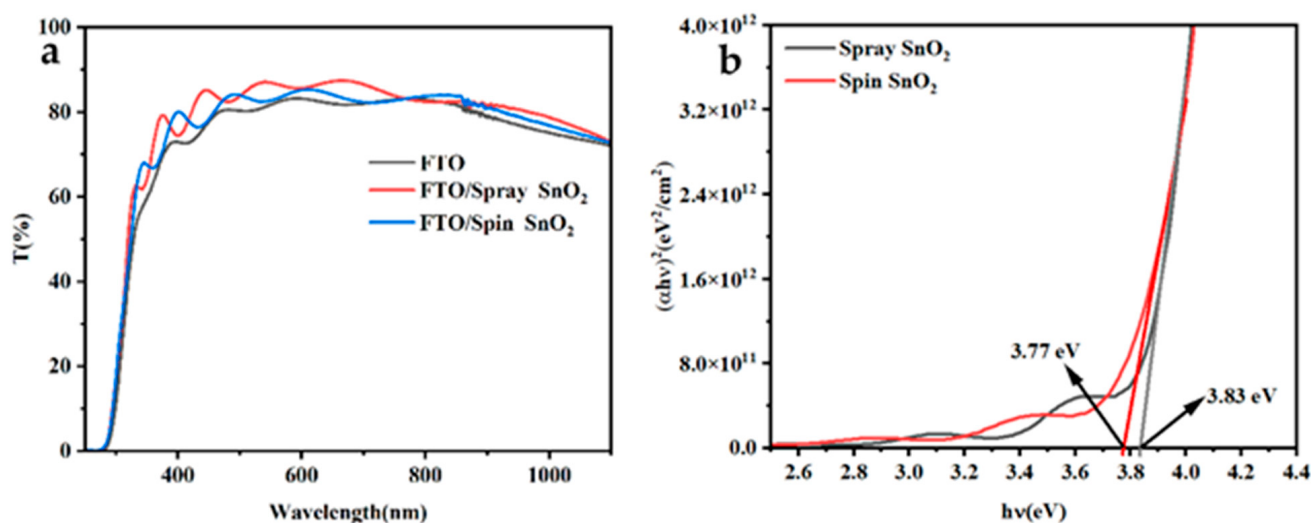
The sprayed and spin-coated  $\text{SnO}_2$  films were laser-scribed (Model Laser 300, Wuhan Iridium Kesai Technology Co., Ltd. Wuhan, China) into a template, and the surface was purged with nitrogen to remove the particles left by the laser-scribing. The substrate was exposed to UV–ozone for 15 min. The  $\text{Cs}_{0.06}\text{MA}_{0.1}\text{FA}_{0.84}\text{Pb}(\text{I}_{0.9}\text{Br}_{0.07}\text{Cl}_{0.03})_3$  solution was spin-coated at 3000 rpm for 30 s by one-step method. Antisolvent chlorobenzene was added after 26 s. Then, the substrate was annealed at 120 °C for 40 min. After the substrate was cooled to room temperature, 60  $\mu\text{L}$  of Spiro-OMeTAD solution (72.3 mg Spiro-OMeTAD was dissolved in 1 mL of CB, and then 22  $\mu\text{L}$  of Li-TFSI (520 mg Li-TFSI was dissolved in 1 mL of acetonitrile) and 30  $\mu\text{L}$  of tBP was added as additive) was added to the perovskite layer. Then the solution was spin-coated at 3000 rpm for 30 s. After that, the sample was oxidized overnight (about 12 h) in a low-humidity environment, and finally, a 100 nm thick gold layer was thermally evaporated at a rate of 0.08–0.15 Å/s.

### 2.4. Test and Characterization

The thickness of the  $\text{SnO}_2$  film was tested by KLA Tencor D-600 Stylus Profiler (Shanghai Nateng Instrument Co., Ltd., Shanghai, China). The carrier concentration was obtained by a Hall test system (model LX-2-DM). The transmittance was measured by a PerkinElmer Lambda950 ultraviolet–visible spectrophotometer. The surface of the  $\text{SnO}_2$  film sample was observed by a Bruker atomic force microscope. The XRD data of the  $\text{SnO}_2$  thin film were obtained by a Shimadzu X-ray diffraction-6100 (Shimadzu Corporation, Japan) diffractometer under 40 kV and 30 mA Cu-K $\alpha$  ( $\lambda = 0.15406$  nm) irradiation. Thermo Scientific K-Alpha (Shanghai Yuzhong Industrial Co., Ltd., China) equipment was used to perform XPS testing of the  $\text{SnO}_2$  thin film. The excitation source was Al K $\alpha$  rays ( $h\nu = 1486.6$  eV,  $\lambda = 0.8341$  nm). The vacuum pressure of the analysis chamber was lower than  $5.0 \times 10^{-5}$  Pa. The pass energy of the full-spectrum scan was 100 eV, and the step length was 1 eV. The pass energy of the narrow-spectrum scan was 50 eV, and the step length was 0.05 eV. The J–V curve was measured with a Keysight Technologies B2901A source meter under simulated AM 1.5 G sunlight at 100 mW  $\text{cm}^{-2}$  (1 sunlight). The light intensity was calibrated by a silicon reference cell (SRC-00205, Enli Tech, Guangyan Technology Co., Ltd., Taiwan, China) and a solar simulator (SS-F5-3A, Enli Tech, Guangyan Technology Co., Ltd., Taiwan, China).

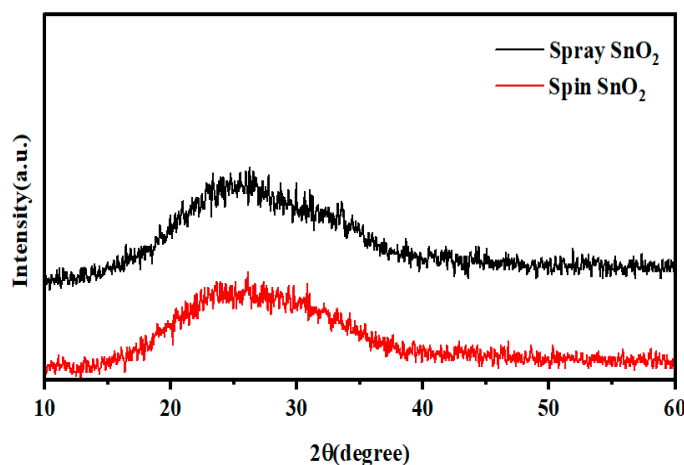
## 3. Results and Discussion

Figure 1 shows the transmission spectra and Tauc diagram of the spin-coated and sprayed  $\text{SnO}_2$  films. The transmission spectra of FTO substrate, spin-coated and sprayed  $\text{SnO}_2$  films in the wavelength range of 250–1100 nm were tested by an ultraviolet spectrophotometer. It can be seen that the transmittance of the  $\text{SnO}_2$  films prepared by spin-coating and spraying are very similar despite the interference of light, and both of them were slightly higher than that of the FTO substrate. The Tauc curves of the films show that the band gap of the  $\text{SnO}_2$  film prepared by spraying was 3.83 eV, which is a bit larger than the 3.77 eV of the  $\text{SnO}_2$  prepared by spin-coating. A larger optical band gap allows more photons to pass through the film, which improves the utilization of light.



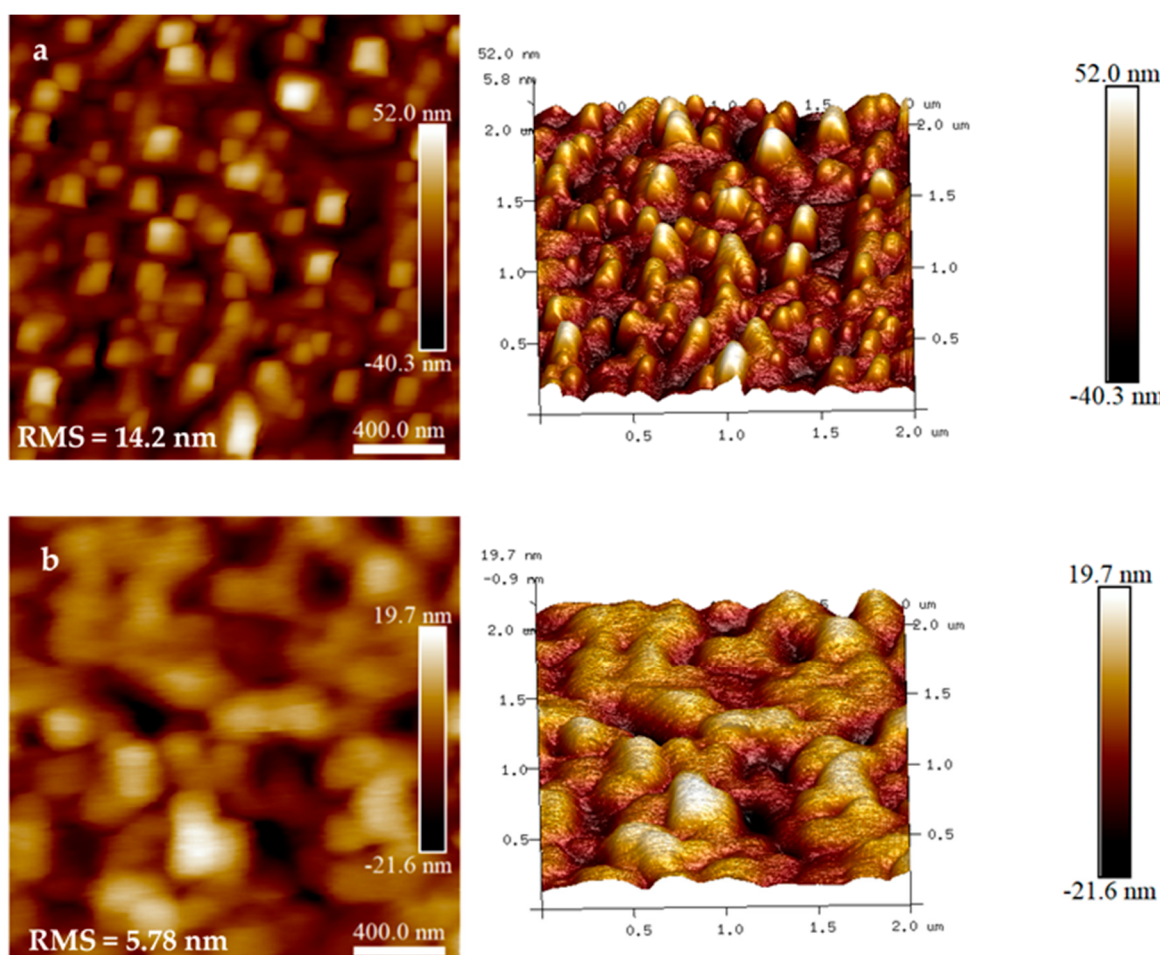
**Figure 1.** Transmission spectrum (a) and Tauc diagram (b) of spin-coated and sprayed SnO<sub>2</sub> films.

Figure 2 shows the XRD patterns of spin-coated and sprayed SnO<sub>2</sub> films on ultra-clear glass (size 45 mm × 60 mm × 1.1 mm, Luoyang Tengjing Glass Co., Ltd. Luoyang, China). The results showed that the SnO<sub>2</sub> films prepared by the two methods were amorphous films.



**Figure 2.** XRD patterns of spin-coated and sprayed SnO<sub>2</sub> films.

In order to study the differences in surface morphology of SnO<sub>2</sub> films prepared by the two methods, we prepared SnO<sub>2</sub> films with thickness of 20 nm on the FTO substrate by spin-coating and spraying, respectively. The AFM test results of the films are shown in Figure 3. The root-mean-square roughness (RMS) of the film prepared by the spin-coating is 14.2 nm and the maximum fluctuation is 92.3 nm, while the RMS of the film prepared by spraying is 5.78 nm and the maximum fluctuation is 41.3 nm. For the absorption layer of about 500 nm in the perovskite solar cell, if the surface roughness of the SnO<sub>2</sub> film is too large, it may affect the interface between the SnO<sub>2</sub> ETL and the absorption layer, resulting in interfacial charge recombination, and thus reduce the V<sub>OC</sub> and FF.



**Figure 3.** AFM images of spin-coated (a) and sprayed (b)  $\text{SnO}_2$  thin films.

We tested the XPS spectra of  $\text{SnO}_2$  films prepared by spin-coating and spray. The fit of each peak was represented by the sum of Gaussian (70%) and Lorentz (30%) lines, and the secondary electron background was subtracted by the Sherry function (yellow line in the figure). Figure 4 shows XPS spectra of spin-coated and sprayed  $\text{SnO}_2$  films. It can be seen from Figure 4a that the elements contained in both films are Sn and O. The binding energies of the O-Sn<sup>2+</sup> and O-Sn<sup>4+</sup> peaks were 530.1 eV and 530.6 eV, respectively [25]. The 532.43 eV peak of the spin-coated film and the 531.6 eV peak of the sprayed film could be the peak of C=O and the peak of O<sub>2</sub> adsorption [26–28]. By fitting the peak area ratio, it can be obtained that the ratio of O-Sn<sup>2+</sup>/O-Sn<sup>4+</sup> for the spin-coating film is 0.72, and the ratio of O-Sn<sup>2+</sup>/O-Sn<sup>4+</sup> for the spraying film is 0.83. This indicates that the SnO content of the sprayed film is higher, which suggests more oxygen vacancies.

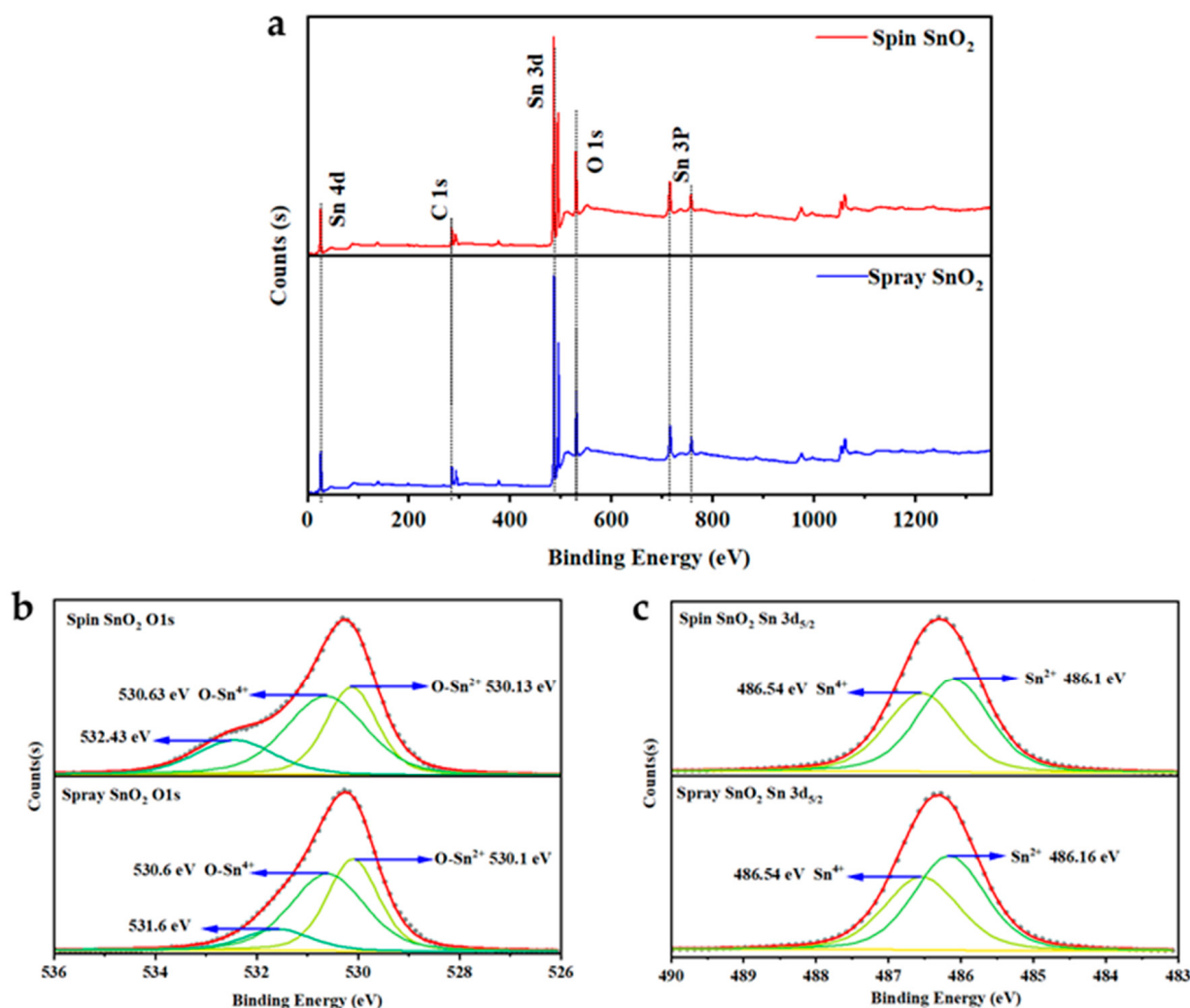


**Figure 4.** XPS spectra of spin-coated and sprayed SnO<sub>2</sub> films: (a) full spectra, (b) high-resolution O1s spectra, (c) high-resolution Sn3d spectra.

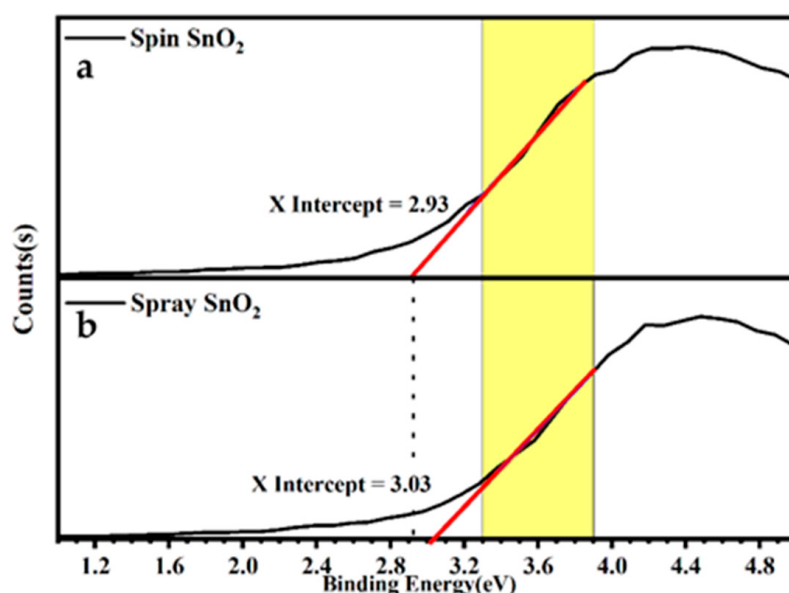
The Sn3d spectra both for the spin-coated and sprayed films are almost the same, which show two peaks at 486.1 eV and 486.54 eV, corresponding to the binding energy of Sn<sup>2+</sup>-O and Sn<sup>4+</sup>-O, respectively [29]. The integration area of the two peaks reflects the relative amount of Sn<sup>2+</sup>/Sn<sup>4+</sup>. The ratios of Sn<sup>2+</sup>/Sn<sup>4+</sup> of the spin-coated and sprayed film are 1.19 and 1.25, respectively, which suggests that the proportion of Sn<sup>2+</sup> in the sprayed film is higher.

Figure 5 shows the XPS valence band spectrum of spin-coated and sprayed SnO<sub>2</sub> thin films. It can be seen that the distance from the valence-band maximum (E<sub>VBM</sub>) to the Fermi level (E<sub>F</sub>) of the spin-coated film is 2.93 eV, while the sprayed film is 3.03 eV. Since the optical band gaps of them are 3.77 eV and 3.83 eV, respectively, the distance between the E<sub>F</sub> and conduction band minimum (E<sub>CBM</sub>) of the spin-coated film is 0.84 eV, and spin-coated film is 0.80 eV. The carrier concentration can be calculated from the following formula:

$$n_0 = N_C \exp\left(-\frac{E_C - E_F}{k_B T}\right)$$

where  $n_0$  is the carrier concentration,  $N_C$  is the effective density of states in the conduction band,  $E_C$  is the conduction band,  $E_F$  is the Fermi level,  $k_B$  is the Boltzmann constant, and  $T$  is the thermodynamic temperature. Since  $k_B T$  is about 0.026 eV at room temperature, it can be estimated that the carrier concentration ratio of sprayed and spin-coated SnO<sub>2</sub> film is

4.66, which is demonstrated by the Hall effect. We tested 200 nm thick  $\text{SnO}_2$  films from two methods. The results show that the carrier concentration and carrier mobility of the sprayed  $\text{SnO}_2$  film is  $1.0 \times 10^{14} \text{ cm}^{-3}$  and  $65 \text{ cm}^2/\text{Vs}$ , and that of the spin-coated  $\text{SnO}_2$  film is  $1.8 \times 10^{13} \text{ cm}^{-3}$  and  $678 \text{ cm}^2/\text{Vs}$ . This is consistent with the XPS analysis.



**Figure 5.** XPS valence band spectrum of spin-coated (a) and sprayed (b)  $\text{SnO}_2$  films.

Based on spin-coating and spraying methods, we prepared perovskite cells with device structures of FTO/ $\text{SnO}_2$ /PVK/Spiro/Au and compared the performance of the cells prepared by the two methods through light I–V tests. The effective area of the cell was  $0.0975 \text{ cm}^2$ . The whole process is exactly the same except for the  $\text{SnO}_2$  preparation. Figure 6 shows the J–V and EQE curves of the two cells with the highest efficiency among the two types of cells. Figure 7 shows the box-plot of light I–V parameters of the two types of perovskite cells. Cells based on sprayed  $\text{SnO}_2$  film have larger open circuit voltage ( $V_{OC}$ ), higher fill factor (FF), and lower series resistance, which is mainly attributed to the higher carrier concentration of  $\text{SnO}_2$ . High carrier concentration means that the Fermi level is closer to the conduction band minimum, and the chemical potential between the electron and hole transport layer is higher. Therefore, the cells based on sprayed  $\text{SnO}_2$  have higher  $V_{OC}$  and FF. It can be seen that the short-circuit current density ( $J_{SC}$ ) of cells based on spin-coated  $\text{SnO}_2$  were slightly higher from Figure 6 (300–500 nm) and Figure 7d. It might be attributed to the larger surface roughness for the spin-coated  $\text{SnO}_2$  film, resulting in a light trapping effect and increasing the absorption of light by the perovskite film. Because the absorption length for the 300–500 nm light is very short (~55 nm), the rough surface usually has an obvious effect in this range which leads to the EQE improvement. The highest efficiency of the perovskite cell prepared based on the spraying method of  $\text{SnO}_2$  is 0.8% higher than that of the spin-coating method, and the average efficiency is about 1.1% higher due to the lower roughness and higher carrier concentration of  $\text{SnO}_2$ . The ultrasonic spraying method is very suitable for preparing the  $\text{SnO}_2$  ETL on a large-area substrate.

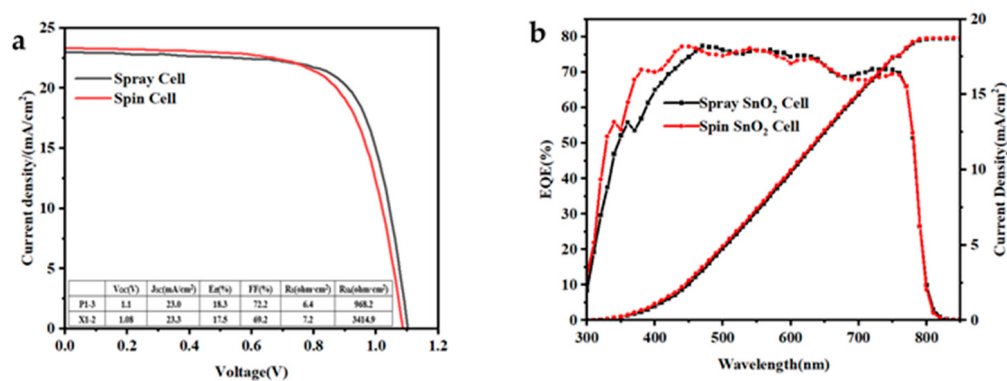


**Figure 6.** J–V (a) and EQE (b) curves of perovskite cell prepared based on sprayed and spin-coated SnO<sub>2</sub> film.

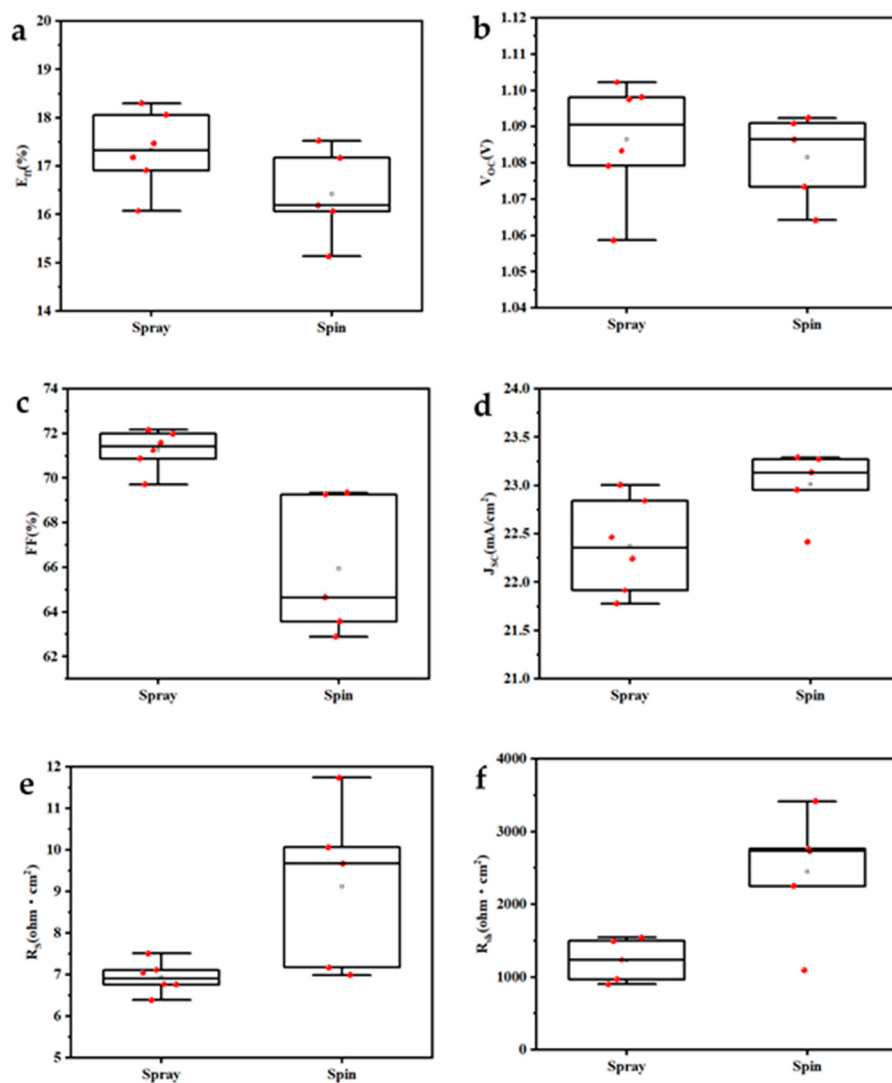


**Figure 7.** Box plot of light I–V parameters of perovskite cells based on sprayed and spin-coated SnO<sub>2</sub> films. (a)  $E_{ff}$ , (b)  $V_{oc}$ , (c) FF, (d)  $J_{sc}$ , (e)  $R_s$ , (f)  $R_{sh}$ .

#### 4. Conclusions

In this paper, SnO<sub>2</sub> film with thickness of about 20 nm was prepared by ultrasonic spraying. Compared with the spin-coated SnO<sub>2</sub> film of the same thickness, the film prepared by spraying has a higher optical transmittance and a wider optical band gap of

3.83 eV. The surface roughness of the film prepared by the spraying method is lower. The carrier concentration of the sprayed film is  $1.0 \times 10^{14} \text{ cm}^{-3}$ , which is slightly higher than that of the spin-coated film. The highest efficiency of the perovskite cell prepared based on the spraying method of  $\text{SnO}_2$  is 0.8% higher than that of the spin-coating method, and the average efficiency is about 1.1% higher due to the lower roughness and higher carrier concentration of  $\text{SnO}_2$ . The ultrasonic spraying method is very suitable for preparing the  $\text{SnO}_2$  ETL on a large-area substrate, so it has greater development potential in the field of flexible perovskite cells.

**Author Contributions:** Conceptualization, L.W. and W.L.; methodology, L.W. and W.L.; software, X.Y.; validation, W.L., A.H. and S.X.; formal analysis, L.W.; investigation, W.L.; data curation, W.L.; writing—original draft preparation, W.L.; writing—review and editing, L.W. and W.L.; supervision, L.W.; project administration, L.W. All authors have read and agreed to the published version of the manuscript.

**Funding:** This research was funded by Sichuan Provincial Department of Science and Technology Project (Research on the Industrialization Process of Ultra-high Purity Metallic Materials (No.2019YFG0513), Research on the high efficiency flexible perovskite module (No.2021YFG0102) and Key technology research and development and industrialization demonstration of perovskite/silicon tandem solar cells (No.2022YFG0121)).

**Institutional Review Board Statement:** Not applicable.

**Informed Consent Statement:** Not applicable.

**Data Availability Statement:** All important data is included in the manuscript.

**Conflicts of Interest:** The authors declare that they have no conflict of interest.

## References

1. Kojima, A.; Teshima, K.; Shirai, Y.; Miyasaka, T. Organometal Halide Perovskites as Visible-Light Sensitizers for Photovoltaic Cells. *J. Am. Chem. Soc.* **2009**, *131*, 6050–6051. [[CrossRef](#)]
2. Jeon, N.J.; Noh, J.H.; Yang, W.S.; Kim, Y.C.; Ryu, S.; Seo, J.; Seok, S.I. Compositional engineering of perovskite materials for high-performance solar cells. *Nature* **2015**, *517*, 476–480. [[CrossRef](#)]
3. Lee, J.-W.; Seol, D.-J.; Cho, A.-N.; Park, N.-G. High-Efficiency Perovskite Solar Cells Based on the Black Polymorph of  $\text{HC}(\text{NH}_2)_2\text{PbI}_3$ . *Adv. Mater.* **2014**, *26*, 4991–4998. [[CrossRef](#)]
4. Green, M.A.; Ho-Baillie, A.; Snaith, H.J. The emergence of perovskite solar cells. *Nat. Photonics* **2014**, *8*, 506–514. [[CrossRef](#)]
5. Kim, H.-S.; Lee, C.-R.; Im, J.-H.; Lee, K.-B.; Moehl, T.; Marchioro, A.; Moon, S.-J.; Humphry-Baker, R.; Yum, J.-H.; Moser, J.E.; et al. Lead Iodide Perovskite Sensitized All-Solid-State Submicron Thin Film Mesoscopic Solar Cell with Efficiency Exceeding 9%. *Sci. Rep.* **2012**, *2*, 591. [[CrossRef](#)]
6. N.E.C. 2021. Available online: <https://www.nrel.gov/pv/cell-efficiency.html> (accessed on 14 December 2021).
7. Xiao, Z.; Song, Z.; Yan, Y. From Lead Halide Perovskites to Lead-Free Metal Halide Perovskites and Perovskite Derivatives. *Adv. Mater.* **2019**, *31*, 1803792. [[CrossRef](#)]
8. Brenner, T.M.; Egger, D.A.; Kronik, L.; Hodges, G.; Cahen, D. Hybrid organic—inorganic perovskites: Low-cost semiconductors with intriguing charge-transport properties. *Nat. Rev. Mater.* **2016**, *1*, 15007. [[CrossRef](#)]
9. Park, N.-G. Research Direction toward Scalable, Stable, and High Efficiency Perovskite Solar Cells. *Adv. Energy Mater.* **2020**, *10*, 1903106. [[CrossRef](#)]
10. Xiong, L.; Guo, Y.; Wen, J.; Liu, H.; Yang, G.; Qin, P.; Fang, G. Review on the Application of  $\text{SnO}_2$  in Perovskite Solar Cells. *Adv. Funct. Mater.* **2018**, *28*, 1802757. [[CrossRef](#)]
11. Tran, V.-H.; Amabde, R.; Ambade, S.; Lee, S.-H.; Lee, I.-H. Low-Temperature Solution-Processed  $\text{SnO}_2$  Nanoparticles as a Cathode Buffer Layer for Inverted Organic Solar Cells. *ACS Appl. Mater. Interfaces* **2017**, *9*, 1645–1653. [[CrossRef](#)]
12. Liu, D.; Wang, Y.; Xu, H.; Zheng, H.; Zhang, T.; Zhang, P.; Wang, F.; Wu, J.; Wang, Z.; Chen, Z.; et al.  $\text{SnO}_2$ -Based Perovskite Solar Cells: Configuration Design and Performance Improvement. *Solar RRL* **2019**, *3*, 1800292. [[CrossRef](#)]
13. Yang, G.; Chen, C.; Yao, F.; Chen, Z.; Zhang, Q.; Zheng, X.; Ma, J.; Lei, H.; Qin, P.; Xiong, L.; et al. Effective Carrier-Concentration Tuning of  $\text{SnO}_2$  Quantum Dot Electron-Selective Layers for High-Performance Planar Perovskite Solar Cells. *Adv. Mater.* **2018**, *30*, 1706023. [[CrossRef](#)]
14. Mohamad Noh, M.F.; Arzaee, N.A.; Safaei, J.; Mohamed, N.A.; Kim, H.P.; Mohd Yusoff, A.R.; Jang, J.; Mat Teridi, M.A. Eliminating oxygen vacancies in  $\text{SnO}_2$  films via aerosol-assisted chemical vapour deposition for perovskite solar cells and photoelectrochemical cells. *J. Alloys Compd.* **2019**, *773*, 997–1008. [[CrossRef](#)]

15. Correa Baena, J.P.; Steier, L.; Tress, W.; Saliba, M.; Neutzner, S.; Matsui, T.; Giordano, F.; Jacobsson, T.J.; Srimath Kandada, A.R.; Zakeeruddin, S.M.; et al. Highly efficient planar perovskite solar cells through band alignment engineering. *Energy Environ. Sci.* **2015**, *8*, 2928–2934. [[CrossRef](#)]
16. Bai, G.; Wu, Z.; Li, J.; Bu, T.; Li, W.; Li, W.; Huang, F.; Zhang, Q.; Cheng, Y.-B.; Zhong, J. High performance perovskite sub-module with sputtered SnO<sub>2</sub> electron transport layer. *Sol. Energy* **2019**, *183*, 306–314. [[CrossRef](#)]
17. Ramarajan, R.; Purushothamreddy, N.; Dileep, R.K.; Kovendhan, M.; Veerappan, G.; Thangaraju, K.; Paul Joseph, D. Large-area spray deposited Ta-doped SnO<sub>2</sub> thin film electrode for DSSC application. *Sol. Energy* **2020**, *211*, 547–559. [[CrossRef](#)]
18. Mahmood, K.; Khalid, A.; Nawaz, F.; Mehran, M.T. Low-temperature electrospray-processed SnO<sub>2</sub> nanosheets as an electron transporting layer for stable and high-efficiency perovskite solar cells. *J. Colloid Interface Sci.* **2018**, *532*, 387–394. [[CrossRef](#)]
19. Taheri, B.; Calabò, E.; Matteocci, F.; Di Girolamo, D.; Cardone, G.; Liscio, A.; Di Carlo, A.; Brunetti, F. Automated Scalable Spray Coating of SnO<sub>2</sub> for the Fabrication of Low-Temperature Perovskite Solar Cells and Modules. *Energy Technol.* **2020**, *8*, 1901284. [[CrossRef](#)]
20. Bishop, J.E.; Read, C.D.; Smith, J.A.; Routledge, T.J.; Lidzey, D.G. Fully Spray-Coated Triple-Cation Perovskite Solar Cells. *Sci. Rep.* **2020**, *10*, 6610. [[CrossRef](#)]
21. Wang, Y.; Yang, L.; Dall’Agnese, C.; Chen, G.; Li, A.-J.; Wang, X.-F. Spray-coated SnO<sub>2</sub> electron transport layer with high uniformity for planar perovskite solar cells. *Front. Chem. Sci. Eng.* **2021**, *15*, 180–186. [[CrossRef](#)]
22. Smith, J.; Game, O.; Bishop, J.; Spooner, E.; Kilbride, R.; Greenland, C.; Jayaprakash, R.; Alanazi, T.; Cassella, E.; Tejada, A.; et al. Rapid Scalable Processing of Tin Oxide Transport Layers for Perovskite Solar Cells. *ACS Appl. Energy Mater.* **2020**, *3*, 5552–5562. [[CrossRef](#)] [[PubMed](#)]
23. Guan, J.; Ni, J.; Zhou, X.; Liu, Y.; Yin, J.; Wang, D.; Zhang, Y.; Li, J.; Cai, H.; et al. High-Performance Electron Transport Layer Via Ultrasonic Spray Depositon for Commercialized Perovskite Solar Cells. *ACS Appl. Energy Mater.* **2020**, *3*, 11570–11580. [[CrossRef](#)]
24. Jiang, Q.; Zhao, Y.; Zhang, X.; Yang, X.; Chen, Y.; Chu, Z.; Ye, Q.; Li, X.; Yin, Z.; You, J. Surface passivation of perovskite film for efficient solar cells. *Nat. Photonics* **2019**, *13*, 460–466. [[CrossRef](#)]
25. Moulder, J.F.; Stickle, W.F.; Sobol, W.M.; Bomben, K.D. *Handbook of X-Ray Photoelectron Spectroscopy*; Physical Electronics, Inc.: Eden Prairie, MN, USA, 1992; p. 231.
26. Wang, Y.; Gao, P.; Sha, L.; Chi, Q.; Yang, L.; Zhang, J.; Chen, Y.; Zhang, M. Spatial separation of electrons and holes for enhancing the gas-sensing property of a semiconductor: ZnO/ZnSnO<sub>3</sub> nanorod arrays prepared by a hetero-epitaxial growth. *Nanotechnology* **2018**, *29*, 175501. [[CrossRef](#)] [[PubMed](#)]
27. Petrov, V.V.; Bayan, E.M.; Khubezhov, S.A.; Varzarev, Y.N.; Volkova, M.G. Investigation of Rapid Gas-Sensitive Properties Degradation of ZnO–SnO<sub>2</sub> Thin Films Grown on the Glass Substrate. *Chemosensors* **2020**, *8*, 40. [[CrossRef](#)]
28. Bhangare, B.; Ramgir, N.S.; Jagtap, S.; Debnath, A.K.; Muthe, K.P.; Terashima, C.; Aswal, D.K.; Gosavi, S.W.; Fujishima, A. XPS and Kelvin probe studies of SnO<sub>2</sub>/RGO nanohybrids based NO<sub>2</sub> sensors. *Appl. Surf. Sci.* **2019**, *487*, 918–929. [[CrossRef](#)]
29. Hu, J.; Tu, J.; Li, X.; Wang, Z.; Yan, L.; Li, Q.; Wang, F. Enhanced UV-Visible Light Photocatalytic Activity by Constructing Appropriate Heterostructures between Mesopore TiO<sub>2</sub> Nanospheres and Sn<sub>3</sub>O<sub>4</sub> Nanoparticles. *Nanomaterials* **2017**, *7*, 336. [[CrossRef](#)]